

Structures and Templating Effect in the Formation of 2D Layered Aluminophosphates with $\text{Al}_3\text{P}_4\text{O}_{16}^{3-}$ Stoichiometry

Jiyang Li, Jihong Yu, Wenfu Yan, Yihua Xu, Wenguo Xu, Shilun Qiu, and Ruren Xu*

Key Laboratory of Inorganic Synthesis and Preparative Chemistry, Jilin University, Changchun 130023, P. R. China

Received May 13, 1999. Revised Manuscript Received June 29, 1999

The structural features of a family of layered aluminophosphates with $\text{Al}_3\text{P}_4\text{O}_{16}^{3-}$ stoichiometry (denoted **L-n**) have been discussed. Their 2D sheets are stabilized by protonated organic amines through H-bonding interactions with certain regularity. The templating ability of various organic amines for the experimental inorganic layers is investigated in terms of the energies of the host–template interactions. Some experimental phenomena, such as the packing sequence of the inorganic layers and the co-templating role of two types of templates on the formation of some structures, can be explained by energy calculation results. Some organic templates that can potentially direct the formation of a given host can be predicted. This further assists in the rational synthesis of 2D layered compounds with specific structures.

Introduction

Molecular sieves have been extensively studied because of their widespread applications in catalysis, ion exchange, and gas separation, as well as in advanced materials and host–guest assembly chemistry. Aluminosilicate zeolites are the well-known family of molecular sieves, which are composed of vertex-sharing TO_4 (T = Si or Al) to produce negatively charged open frameworks with various architectures. Wilson et al. first discovered a family of microporous aluminophosphates, denoted $\text{AlPO}_4\text{-}n$, which are constructed from a strict alternation of AlO_4 and PO_4 tetrahedra in 1982.^{1,2} Some of these materials and their heteroatom-substituted analogues are isostructural with known aluminosilicate zeolites, whereas many compounds exhibit novel structures. The synthesis of microporous aluminophosphates typically involves the crystallization of aluminophosphate gel under hydrothermal or solvothermal conditions, in which the organic amine is used

as a structure-directing agent. Recently, many more compounds, especially aluminophosphates with an Al/P ratio lower than unity, have been synthesized in a variety of structural architectures, showing a more diverse chemistry than their analogues the aluminosilicates. These compounds have been prepared with 3D open framework,^{3,4} 2D layered,^{5–23} and 1D chain^{24–26} structures, of which the 2D layered compounds exhibit rich structural and compositional diversity.

(1) Wilson, S. T.; Lok, B. M.; Messina, C. A.; Cannon, T. R.; Flanigen, E. M. *ACS Symp. Ser.* **1983**, 218, 79.

(2) Wilson, S. T.; Lok, B. M.; Messina, C. A.; Cannon, T. R.; Flanigen, E. M. *J. Am. Chem. Soc.* **1982**, 104, 1146.

(3) (a)Huo, Q.; Xu, R.; Li, S.; Ma, Z.; Thomas, J. M.; Jones, R. H.; Chippindale, A. M. *J. Chem. Soc., Chem. Commun.* **1992**, 875. (b) Jones, R. H.; Thomas, J. M.; Chen, J.; Xu, R.; Huo, Q.; Li, S.; Ma, Z.; Chippindale, A. M. *J. Solid State Chem.* **1993**, 102, 204.

(4) Yu, J.; Sugiyama, K.; Zheng, S.; Qiu, S.; Chen, J.; Xu, R.; Sakamoto, Y.; Terasaki, O.; Hiraga, K.; Light, M.; Hursthouse, M. B.; Thomas, J. M. *Chem. Mater.* **1988**, 10, 1208.

(5) Jones, R. H.; Thomas, J. M.; Xu, R.; Huo, Q.; Cheetham, A. K.; Powell, A. V. *J. Chem. Soc., Chem. Commun.* **1991**, 1266.

(6) Gao, Q.; Li, B.; Chen, J.; Li, S.; Xu, R. *J. Solid State Chem.* **1997**, 129, 37.

(7) Chippindale, A. M.; Natarajan, S.; Thomas, J. M.; Jones, R. H. *J. Solid State Chem.* **1994**, 111, 18.

(8) Jones, R. H.; Chippindale, A. M.; Natarajan, S.; Thomas, J. M. *J. Chem. Soc., Chem. Commun.* **1994**, 565.

(9) Togashi, N.; Yu, J.; Zheng, S.; Sugiyama, K.; Hiraga, K.; Terasaki, O.; Yan, W.; Qiu, S.; Xu, R. *J. Mater. Chem.* **1998**, 8, 2827.

(10) Oliver, S.; Kuperman, A.; Lough, A.; Ozin, G. A. *Inorg. Chem.* **1996**, 35, 6373.

(11) Thomas, J. M.; Jones, R. H.; Xu, R.; Chen, J.; Chippindale, A. M.; Natarajan, S.; Cheetham, A. K. *J. Chem. Soc., Chem. Commun.* **1992**, 929.

(12) Chippindale, A. M.; Cowley, A. R.; Huo, Q.; Jones, R. H.; Law, A. D. *J. Chem. Soc., Dalton Trans.* **1997**, 2639.

(13) Williams, I. D.; Gao, Q.; Chen, J.; Ngai, L.-Y.; Lin, Z.; Xu, R. *Chem. Commun.* **1996**, 1781.

(14) Yu, J.; Li, J.; Sugiyama, K.; Togashi, N.; Terasaki, O.; Hiraga, K.; Zhou, B.; Qiu, S.; Xu, R. *Chem. Mater.* **1999**, 11, 1727.

(15) Yao, Y.; Natarajan, S.; Chen, J.; Pang, W. *J. Solid State Chem.* **1999**, in press.

(16) Morgan, K.; Gainsford, G.; Milestone, N. *J. Chem. Soc., Chem. Commun.* **1995**, 425.

(17) (a)Yu, J.; Williams, I. D. *J. Solid State Chem.* **1998**, 136, 141. (b) Yu, J.; Terasaki, O.; Williams, I. D.; Qiu, S.; Xu, R. *Supramol. Sci.* **1998**, 5, 297.

(18) Chippindale, A. M.; Powell, A. V.; Bull, L. M.; Jones, R. H.; Cheetham, A. K.; Thomas, J. M.; Xu, R. *J. Solid State Chem.* **1992**, 96, 199.

(19) Yu, J.; Sugiyama, K.; Hiraga, K.; Togashi, N.; Terasaki, O.; Tanaka, Y.; Nakata, S.; Qiu, S.; Xu, R. *Chem. Mater.* **1998**, 10, 3636.

(20) Oliver, S.; Kuperman, A.; Lough, A.; Ozin, G. A. *Chem. Commun.* **1996**, 1761.

(21) Oliver, S.; Kuperman, A.; Lough, A.; Ozin, G. A. *Chem. Mater.* **1996**, 8, 2391.

(22) Morgan, K. R.; Gainsford, G. J.; Milestone, N. B. *Chem. Commun.* **1997**, 61.

(23) Vidal, L.; Gramlich, V.; Patarin, J.; Gabelica, Z. *Eur. J. Solid State Chem.* **1998**, 35, 345.

(24) Gao, Q.; Chen, J.; Li, S.; Xu, R.; Thomas, J. M.; Light, M.; Hursthouse, M. B. *J. Solid State Chem.* **1996**, 127, 145.

(25) Williams, I. D.; Yu, J.; Gao, Q.; Chen, J.; Xu, R. *Chem. Commun.* **1997**, 1273.

(26) Jones, R. H.; Thomas, J. M.; Xu, R.; Huo, Q.; Xu, Y.; Cheetham, A. K.; Bieber, D. *J. Chem. Soc., Chem. Commun.* **1990**, 1170.

Table 1. 2D Layered Aluminophosphates with $\text{Al}_3\text{P}_4\text{O}_{16}^{3-}$ Stoichiometry^a

L-n	formula	structure feature	stacking sequence	SBU	ref(s)
L-1	$[\text{Al}_3\text{P}_4\text{O}_{16}][\text{NH}_3(\text{CH}_2)_2\text{NH}_3][\text{OH}_2(\text{CH}_2)_2\text{OH}][\text{OH}(\text{CH}_2)_2\text{OH}]$	4.6.8(a)-net	ABAB	SBU1	5
L-2	$[\text{Al}_3\text{P}_4\text{O}_{16}]3[\text{CH}_3\text{CH}_2\text{NH}_3]$	4.6.8(a)-net	AAAA	SBU1	6
L-3	$[\text{Al}_3\text{P}_4\text{O}_{16}][\text{NH}_3(\text{CH}_2)_5\text{NH}_3][\text{C}_5\text{H}_{10}\text{NH}_2]$	4.6.8(a)-net	AAAA	SBU1	7, 8
L-4	$[\text{Al}_3\text{P}_4\text{O}_{16}]3[\text{CH}_3\text{CH}_2\text{CH}_2\text{NH}_3]$	4.6.8(a)-net	AAAA	SBU1	9
L-5	$[\text{Al}_3\text{P}_4\text{O}_{16}][\text{C}_5\text{H}_{10}\text{NH}_2]2[\text{C}_4\text{H}_7\text{NH}_3]$	4.6.8(a)-net	AAAA	SBU1	10
L-6	$[\text{Al}_3\text{P}_4\text{O}_{16}]1.5[\text{NH}_3(\text{CH}_2)_4\text{NH}_3]$	4.6.12-net	ABAB	SBU1	11
L-7	$[\text{Al}_3\text{P}_4\text{O}_{16}]3[\text{CH}_3(\text{CH}_2)_3\text{NH}_3]$	4.6.12-net	AAAA	SBU1	12
L-8	$[\text{Al}_3\text{P}_4\text{O}_{16}]1.5[\text{NH}_3\text{CHCH}_3\text{CH}_2\text{NH}_3]0.5[\text{H}_2\text{O}]$	4.6(a)-net	ABAB	SBU2	13
L-9	$[\text{Al}_3\text{P}_4\text{O}_{16}]2[\text{C}_5\text{N}_2\text{H}_9][\text{NH}_4]$	4.6(b)-net	AAAA	SBU3	14
L-10	$[\text{Al}_3\text{P}_4\text{O}_{16}][\text{TETAH}_3]$	4.6.8(b)-net	ABAB	SBU3	15
L-11	$[\text{Al}_3\text{P}_4\text{O}_{16}][\text{Co}(\text{en})_3]3\text{H}_2\text{O}$	4.6(c)-net	ABAB	SBU4	16

^a Abbreviations: TETA, $\text{NH}_2\text{CH}_2\text{CH}_2\text{NHCH}_2\text{CH}_2\text{NHCH}_2\text{CH}_2\text{NH}_2$; SBU1, capped 6-MR; SBU2, double diamond SBU; SBU3, branched double edge sharing 4-MR; SBU4, the Al_3P_2 trigonal-bipyrimidal core.

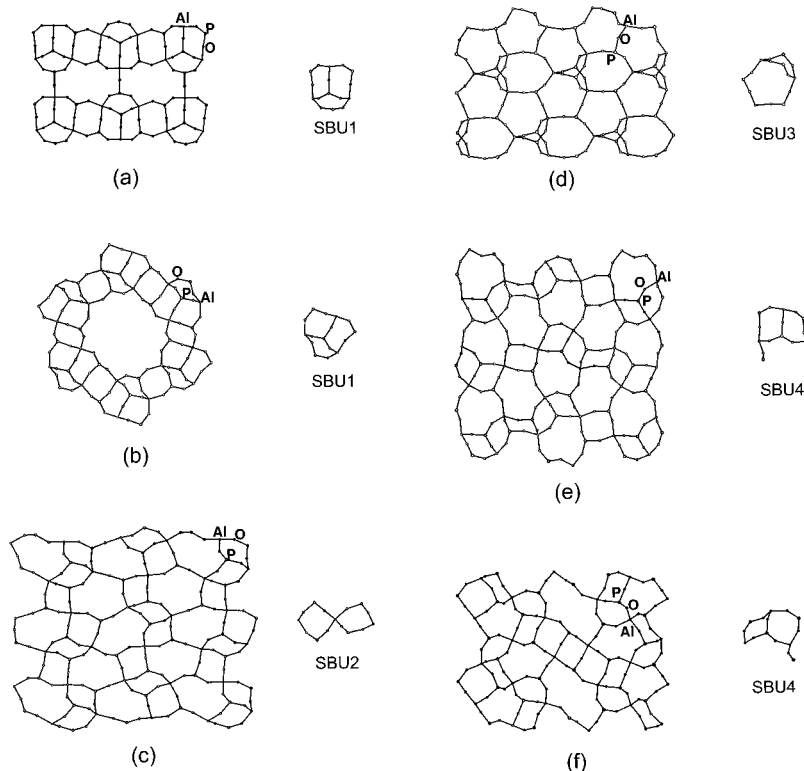


Figure 1. The topologies and secondary building units (SBU) of six distinct 2D networks of L-n: (a) 4.6.8(a)-net, (b) 4.6.12-net, (c) 4.6(a)-net, (d) 4.6(b)-net, (e) 4.6(c)-net, and (f) 4.6.8(b)-net.

The synthesis chemistry of these materials is very complex. One reason is that microporous compounds and related materials are kinetic rather than thermodynamic crystalline products; another reason is that the crystallization process is manipulated by various factors, such as the solvent, the gel composition, the type of templates, crystallization time, and crystallization temperature. Therefore, achieving a rational synthesis of target materials becomes more difficult. A large proportion of recent work has focused on elucidating the mechanism of formation of microporous compounds. However, the mechanism of synthesis is still poorly understood now. Nonetheless, template agents are believed to have significant influence on the final structure of microporous materials through the following templating roles: (1) space-filling, (2) structure-directing, and (3) true templating.²⁷ Recently, much attention has been focused on the structure-directing effect of the size and shape of organic amines, notable

examples being the successful synthesis of SSZ-24 and DAF-1 by careful preselection of a specific organic species which results in channels of the desired size.^{28,29} On the other hand, Xu and co-workers have considered the templating ability on the basis of steric–electronic effects.^{30,31} Catlow et al. has developed methodologies to determine the relative templating efficacy of an organic species within a large range of known zeolite frameworks in terms of nonbonding interaction between templates and host.³²

We now concentrate our efforts to investigate the templating ability for the formation of a family of 2D

(28) Zones, S. I.; Yuen, L. T.; Nakagawa, Y.; van Nordstrand, R. A.; Toto, S. D. In *Proceedings of 9th International Zeolites Conference*; Butterworth-Heinemann: Montreal, 1992.

(29) Wright, P. A.; Jones, R. H.; Natarajan, S.; Bell, R. G.; Chen, J.; Hursthouse, M. B.; Thomas, J. M. *J. Chem. Soc., Chem. Commun.* **1993**, 1861.

(30) Liu, Z.; Xu, R. *Stud. Surf. Sci. Catal.* **1997**, *105*, 405.

(31) Liu, Z.; Xu, W.; Yang, G.; Xu, R. *Microporous Mesoporous Mater.* **1998**, *22*, 33.

(32) Lewis, D. W.; Freeman, C. M.; Catlow, C. R. A. *J. Phys. Chem.* **1995**, *99*, 11194.

(27) Davis, M. E.; Lobo, R. F. *Chem. Mater.* **1992**, *4*, 756.

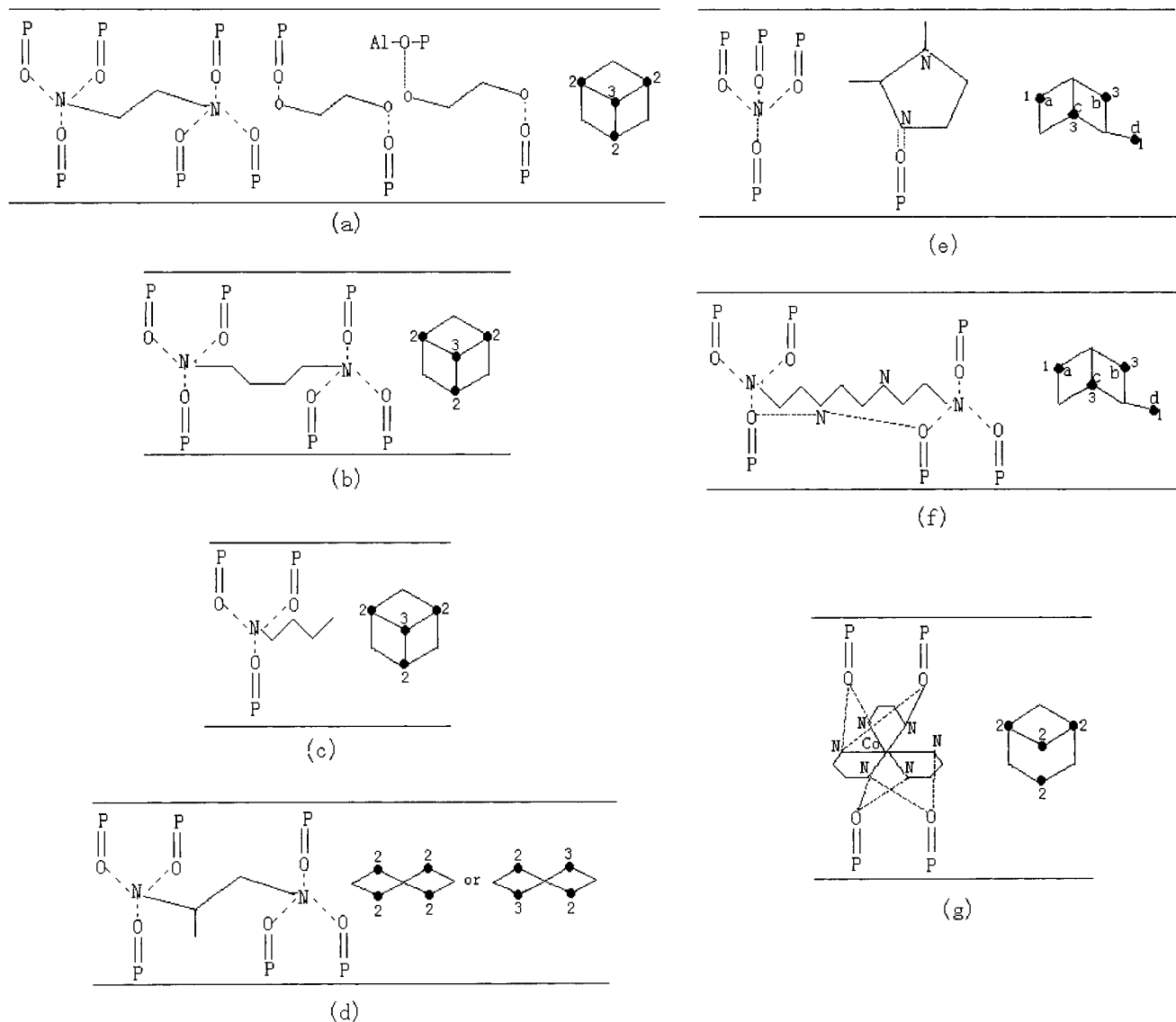


Figure 2. Schematic representation of the interaction of templates–host inorganic layers, (a) **L-1**, (b) **L-6**, (c) **L-7**, (d) **L-8**, (e) **L-9**, (f) **L-10**, and (g) **L-11** (the number of H-bonds provided by the templates to each SBU is indicated by 1, 2, 3; the horizontal lines indicate the layers).

layered aluminophosphates. These compounds are most interesting target materials due to their unique role in the formation of 3D microporous compounds.³³ Moreover, the template interacts with the host inorganic network through H-bonding interaction with certain regularity. This presents a favorable situation for studying the templating effect. In this paper, a family of 2D aluminophosphates with $\text{Al}_3\text{P}_4\text{O}_{16}^{3-}$ stoichiometry is our main concern. Their inorganic layers consist of alternating AlO_4 and $\text{PO}_3(=\text{O})$ tetrahedra and are stabilized by the template molecules located in the interlayer region. A methodology is developed to investigate the templating ability in terms of the interaction energy of host–guest. This methodology will serve as a useful guide in the rational synthesis of the target materials with specific structures and properties.

Methodology of Investigating the Templating Ability

A. The Force Field and Parameter. Our calculation is based on the Burchart 1.01–Dreiding 2.21 force

field that combines the Burchart force field,³⁴ which is used to treat the frameworks of zeolites, and Dreiding II force field,³⁵ which is used to treat the intra- and intermolecular interactions. Because the $\text{P}=\text{O}$ bond type of 2D layered aluminophosphates is not addressed in the force field, some parameters are added according to the references.^{36,37} Upon examination of the experimental structures studied in this work, it was found that the average $\text{P}=\text{O}$ bond length is about 1.495 Å, and $\text{O}=\text{P}=\text{O}$ bond angles are 108.5–116.8°, which does not change much compared to the $\text{O}=\text{P}=\text{O}$ bond angle of 109° of PO_4 tetrahedra. On the basis of these observations parameters of bond energy for $\text{P}=\text{O}$: $R_0 = 1.495$

(33) Oliver, S.; Kuperman, A.; Ozin, G. A. *Angew. Chem., Int. Ed. Engl.* **1998**, *37*, 46.

(34) de Vos Burchart, E. Studies on Zeolites: Molecular Mechanics, Framework Stability and Crystal Growth. Ph.D. Thesis, Technische Universiteit Delft, 1992.

(35) Mayo, S. L.; Olafson, B. D.; Goddard, W. A. *J. Phys. Chem.* **1990**, *94*, 8897.

(36) de Vos Burchart, E.; van Bekkum, H.; van de Graaf, B.; Vogt, E. T. C. *J. Chem. Soc., Faraday Trans.* **1992**, *88*, 2761.

(37) Cerius2, Molecular simulations/Biosym corporation, 1995.

Table 2. Experimental E_s and Its Components per $\text{Al}_3\text{P}_4\text{O}_{16}^{3-}$ Unit (kcal/mol)

L-n	bonds	Urey–Bradley	VDW	electrostatic	E_s	note
L-1	-2681.10	2.50	-13.61	-34.04	-2726.28	4.6.8(a)-net, ABAB
L-2	-2682.77	2.72	-13.44	-34.16	-2727.65	4.6.8(a)-net, AAAA
L-3	-2681.53	3.20	-12.67	-32.22	-2723.20	4.6.8(a)-net, AAAA
L-4	-2683.48	5.49	-12.68	-32.18	-2722.85	4.6.8(a)-net, AAAA
L-5	-2680.79	3.49	-12.46	-32.17	-2721.93	4.6.8(a)-net, AAAA
L-6	-2681.58	2.45	-13.39	-35.60	-2728.13	4.6.12-net, ABAB
L-7	-2682.29	2.54	-12.54	-35.62	-2727.88	4.6.12-net, AAAA
L-8	-2643.21	224.31	-14.08	-31.72	-2465.34	4.6(a)-net, ABAB
L-9	-2681.78	2.92	-13.40	-32.17	-2724.43	4.6(b)-net, AAAA
L-10	-2669.38	12.01	-13.81	-31.81	-2703.00	4.6.8(b)-net, ABAB
L-11	-2667.28	22.44	-14.51	-35.78	-2695.13	4.6(c)-net, ABAB

Table 3. Experimental Interaction Energies of Templates–Inorganic Sheets (E_{inter}) per $\text{Al}_3\text{P}_4\text{O}_{16}^{3-}$ Unit (kcal/mol) and the Interlayer Spacing D (Å)

L-n	D	VDW	H-bond	E_{inter}^a	note
L-1	8.852	15.36	-31.71	-16.36	4.6.8(a)-net, ABAB
L-2	9.363	9.75	-26.50	-16.75	4.6.8(a)-net, AAAA
L-3	9.801	8.20	-25.58	-17.38	4.6.8(a)-net, AAAA
L-4	9.597	-6.02	-27.20	-33.22	4.6.8(a)-net, AAAA
L-6	9.207	18.99	-30.48	-11.49	4.6.12-net, ABAB
L-7	9.633	14.08	-28.99	-14.91	4.6.12-net, AAAA
L-8	7.368	17.13	-21.64	-4.51	4.6(a)-net, ABAB
L-9	10.402	1.88	-20.58	-18.68	4.6(b)-net, AAAA
L-10	9.955	2.33	-16.53	-14.20	4.6.8(b)-net, ABAB
L-11	10.797	17.60	-21.70	-4.10	4.6(c)-net, ABAB

^a The E_{inter} value of L-5 is not calculated due to the unavailable H coordinates

and $D_0 = 87.3428$ were added in the force field. Other parameters are the same as those used in Burchart 1.01–Dreiding2.21 force field given in the Cerius² package.³⁷

B. Building Models. The structural models of experimental 2D layered aluminophosphates are built up according to their crystal structure data using Cerius² package. The procedure of adding various templates to the experimental sheets involves the following (i) choose several experimental sheets as hosts to add theoretical templates—to make the study easier, the unit cell was first fixed for every structure mainly through fixing the interlayer spacing for structures with the same inorganic layers; (ii) decrease their crystal symmetries to $P1$ in order to fit all kinds of organic molecules; (iii) determine the number of the template molecules in one unit cell based on charge balance; and (iv) define the N-atom at the position which is favorable to form H-bond to terminal P=O group, then add the C-atoms. Finally, H-atoms are added and the H-bonding distance (H \cdots O distance) used in this work is 2.2 Å.

C. Energy Calculation. In this paper, we shall mainly study the steric energies (E_s) of inorganic sheets and the interaction energies (E_{inter}) between the inorganic sheets and organic templates. The steric energy includes four kinds of energies: bonds, Urey–Bradley, van der Waals (VDW), and electrostatic energies. The interaction energy between the host and template molecules studied in this work is mainly VDW and H-bonding energies. Since the low-energy nonbonding host–guest interactions, i.e., VDW and H-bonding interactions, can give prominence to the characters of various templates, the Coulombic interactions between the framework and the template are omitted in the calculation.³² The energies of experimental structures are calculated based on experimental structural data. Since 2D layered aluminophosphates, like zeolitic ma-

Table 4. Interlayer Spacing (D) and Interaction Energy of Host–Template Compared with Experimental Data (kcal/mol)

template	D (Å)	VDW	H-bond	E_{inter}
L-2 _(exp)	9.363	9.75	-26.50	-16.75
L-2 _(opt)	9.717	-16.10	-17.02	-33.11
L-2 _(test1)	9.849	-15.46	-17.50	-32.97
L-2 _(test2)	9.765	-18.18	-11.89	-30.07

terials, are thermodynamically metastable phase, further energy optimization was carried out by using energy minimization to roughly optimize the structure first and then the Anneal Dynamics-NPH ensembles of Molecular Dynamics^{38–41} were used to make global optimization. The parameters of Anneal Dynamics used were the default data in the Cerius² package. To obtain more precise results, a multicycle calculation method was adopted, i.e., the calculation was not considered to have been completed until the difference of the last two calculated total energies of the whole structure was lower than 1 kcal/mol.

Results and Discussion

A. Structural Features of the Inorganic Sheets of L-n. Compounds L-n ($n = 1–11$) listed in Table 1 all consist of macroanionic sheets $\text{Al}_3\text{P}_4\text{O}_{16}^{3-}$ that are charge balanced by various protonated organic amines that are located between the layers. The inorganic sheets are constructed from alternating AlO_4 and PO_4 tetrahedra in which all the vertexes of AlO_4 but only three-quarters of the PO_4 are shared and the remaining vertex is a P=O group. Some of L-n possess the same inorganic sheet but differ by the template molecules or the stacking sequence of the layers. The topologies and secondary building units (SBU) of some 2D networks of L-n are given in Figure 1a–f, which represent six distinct 2D nets, i.e., 4.6.8(a)-, 4.6.12-, 4.6(a)-, 4.6(b)-, 4.6(c), and 4.6.8(b)-nets. These 2D sheets are found to stack either in an AAAA or an ABAB sequence. The capped six-membered ring (MR) (SBU1), double diamond (SBU2), branched double edge sharing 4-MR (SBU3), and Al_3P_2 trigonal-bipyrimidal core (SBU4) are found to be the secondary building unit to construct these 2D networks.

B. H-Bonding Interactions between Inorganic Networks and the Templates. The organic amines

(38) Alder, B. J.; Wainwright, T. E. *J. Chem. Phys.* **1957**, *27*, 1208.

(39) Allden, M. P.; Tildesley, D. J. *Computer Simulation of Liquids*; Clarendon Press: Oxford, 1987.

(40) *Computer simulations in Chemical Physics*; Allen, M. P., Tildesley, D. J., Eds; Kluwer Dordrecht: 1994.

(41) Demontis, P.; Suffritti, G. B. In *Modelling of Structure and Reactivity in Zeolites*; Catlow, C. R. A., Ed; Academic Press: London, 1992.

Table 5. Interaction Energies (E_{inter}) of Templates–Inorganic Sheets Per $[\text{Al}_3\text{P}_4\text{O}_{16}]^{3-}$ Unit (kcal/mol)^a

code	template	L-7 (4.6.12, A)	L-6 (4.6.12, B)	L-2 (4.6.8a, A)	L-1 (4.6.8a, B)	L-10 (4.6.8b, B)	L-8 (4.6a, B)	L-11 (4.6c, B)
T-1	C ₂ H ₅ NH ₂	–26.66	–26.33	–33.11	–30.64	–25.12	–25.05	–28.86
T-2	C ₃ H ₇ NH ₂	<i>–32.36</i>	<i>–27.77</i>	<i>–33.27</i>	<i>–25.38</i>	<i>–21.83</i>	<i>–22.39</i>	<i>–25.64</i>
T-3	CH ₃ CH(CH ₃)CH ₂ NH ₂	–28.99	–27.25	<i>–30.78</i>	–22.96	–25.19	–21.13	<i>–32.47</i>
T-4	C ₄ H ₉ NH ₂	–37.07	<i>–29.16</i>	–28.69	28.91	–25.53	–21.62	–23.72
T-5	H ₂ NC ₂ H ₄ NH ₂	–17.85	–18.25	–23.26	–24.68	–28.28	–23.36	–22.71
T-6	H ₂ NCHCH ₃ CH ₂ NH ₂	–21.22	–21.32	–23.31	–17.00	<i>–29.11</i>	–29.02	–26.32
T-7	H ₂ NC ₃ H ₆ NH ₂	–19.02	–19.66	–22.30	–22.68	–21.28	–23.57	–13.19
T-8	H ₂ NCH ₂ CH(CH ₃)CH ₂ NH ₂	–23.87	<i>–29.47</i>	–23.08	–27.48	–21.61	–26.11	–22.15
T-9	H ₂ NC ₄ H ₈ NH ₂	–22.18	–32.54	–22.00	–20.57	–23.89	–24.03	–21.21
T-10	H ₂ NC ₅ H ₁₀ NH ₂	–22.49	–26.83	–25.33	–20.85	–21.69	–23.13	–25.91
T-11	C ₅ H ₁₀ NH ₂	–27.85	–22.37	–28.60	<i>–29.98</i>	–21.78	–17.98	–23.74
T-12	C ₆ N ₄ H ₁₈	<i>–29.14</i>	<i>–29.85</i>	–13.17	–27.76	–30.94	–29.84	–26.21
T-13	H ₂ N(CH ₂) ₆ NH ₂	–23.16	–24.85	<i>–31.68</i>	–21.26	–20.23	–22.49	–22.87
T-14	H ₂ NC ₅ H ₁₀ NH ₂ :C ₅ H ₁₀ NH			<i>–36.36</i>				
T-15	C ₄ H ₇ NH ₂			–21.63				
T-16	C ₅ H ₁₀ NH:2 C ₄ H ₇ NH ₂			<i>–34.38</i>				
T-17	Co(en) ₃							–31.36
T-18	H ₂ NC ₂ H ₄ NH ₂ :2(CH ₂ OH) ₂				–36.88			

^a The experimental templates are emboldened; templates predict as suitable template are italicized. A is AAAA stacking sequence and B is ABAB stacking sequence.

directing the formation of the 2D $\text{Al}_3\text{P}_4\text{O}_{16}^{3-}$ sheets include monoamines, such as $\text{CH}_3\text{CH}_2\text{NH}_2$, $\text{CH}_3\text{CH}_2\text{CH}_2\text{NH}_2$, and $\text{CH}_3\text{CH}_2\text{CH}_2\text{CH}_2\text{NH}_2$, diamines, such as $\text{NH}_2(\text{CH}_2)_2\text{NH}_2$, $\text{NH}_2(\text{CH}_2)_4\text{NH}_2$, and $\text{NH}_2(\text{CH}_2)_6\text{NH}_2$, and cycloamines, such as piperidine, cyclobutylamine, and 1,2-dimethylimidazole. In the formation of **L-11**, $\text{Co}(\text{en})_3$ was used as a template. Variation of the template can result in a different network, as well as a different stacking sequence for layered AlPOs. On the other hand, different templates can direct the formation of the same inorganic layer structure. The protonated template cations, except for balancing the charge of the macroanionic layers, interact with the host inorganic layers (i.e., terminal $\text{P}=\text{O}$) through extensive H-bondings, which is believed to stabilize the whole 2D layered structure. The H-bonding distance ($\text{N}-\text{H}\cdots\text{O}$) in these 2D $\text{Al}_3\text{P}_4\text{O}_{16}^{3-}$ structures is typically in the range of 2.6–2.9 Å. We find that the interaction between the host inorganic network and the template can be well described as the interaction between the secondary building unit (SBU) and the protonated amino groups.

1. Capped 6-MR SBU. Compounds **L-n** ($n = 1-7$) are all featured by capped 6-MR SBU. In **L-1** containing a 4.6.8(a)-net, diprotonated ethylenediamine and monoprotonated ethylene glycol cations both act as H-bond donors to the host networks (Figure 2a). One $\text{OH}(\text{CH}_2)_2\text{OH}_2^+$, one $\text{OH}(\text{CH}_2)_2\text{OH}$, and one $^+\text{NH}_3(\text{CH}_2)_2\text{NH}_3^+$ cation provide a total of nine H-bonds to each SBU. On the other hand, in each SBU, the capping $\text{P}=\text{O}$ group accepts three H-bonds and the other three $\text{P}=\text{O}$ groups each accept two H-bonds. **L-n** ($n = 2-5$), which all contain a 4.6.8(a)-net, exhibit a similar H-bonding interaction system to **L-1**. In **L-6** (4.6.12-net), each SBU also accepts nine H-bonds in total from 1.5 protonated 1,4-diaminobutane molecules with the capping $\text{P}=\text{O}$ group accepting three and other three $\text{P}=\text{O}$ groups each accepting two H-bonds (Figure 2b). As for **L-7**, three protonated butylamine cations provide a total of nine H-bonds to each SBU with the capping $\text{P}=\text{O}$ accepting three and other $\text{P}=\text{O}$ each accepting two H-bonds (Figure 2c). These facts indicate that even though the type of templates is different, the nature of H-bonding interactions between the template and the capped 6-MR SBU is identical.

2. Double Diamond SBU. Double diamond SBU is featured in compound **L-8**, which contains a 4.6(a)-net. Three protonated 1,2-diaminopropane molecules provide 18 H-bonds to two SBUs. One of the SBUs accepts eight H-bonds with each $\text{P}=\text{O}$ accepting two H-bonds. Another SBU accepts 10 H-bonds with two $\text{P}=\text{O}$ each accepting two and the other two $\text{P}=\text{O}$ each accepting three H-bonds (Figure 2d).

3. Branched Double Edge Sharing 4-MR SBU. Compounds **L-9** and **L-10** are featured by branched double edge sharing 4-MR SBU. For **L-9** containing a 4.6(b)-net, protonated 1,2-dimethylimidazolium and ammonium cations both act as H-bonding donors to the host network. One ammonium and two 1,2-dimethylimidazolium cations provide a total of eight H-bonds to each SBU. On the other hand, in each SBU (see Figure 2e), the branched $\text{P}=\text{O}$ (site d) and its opposite $\text{P}=\text{O}$ (site a) accept one H-bond each and the other two $\text{P}=\text{O}$ s (sites b and c) accept three H-bonds each. As with **L-9**, in **L-10**, which contains a 4.6.8(b)-net, each SBU also accepts eight H-bonds in total from three N atoms in one triprotonated triethylenetetraamine molecules. Sites a and d accept one H-bond each, sites c and b accept three H-bonds each (Figure 2f).

4. Al_3P_2 Trigonal-Bipyramidal Core SBU. Compound **L-11**, which contains a 4.6(c)-net, is featured by Al_3P_2 trigonal-bipyramidal core SBU. Protonated $\text{Co}(\text{en})_3$ cations act as H-bonding donors to the host network. One $\text{Co}(\text{en})_3$ provides eight H-bonds to each SBU, of which each terminal $\text{P}=\text{O}$ accepts two H-bonds (see Figure 2g).

As is revealed here, the template molecules interact with the host inorganic network with certain regularity, depending on the type of the SBU. This will allow us to locate some suitable templates in a given host inorganic network and further assist in the study of their templating ability for the 2D layered structures.

C. Predicting the Templating Ability in Terms of Interaction Energy of Host–Template. **1. Energy Calculation of Experimental 2D $\text{Al}_3\text{P}_4\text{O}_{16}^{3-}$ Nets.** First the current steric energy E_s of experimental inorganic sheet and the total energy E of the whole structure are determined using the Burchart 1.01–Dreiding 2.21 force field (Coulombic interaction between the template

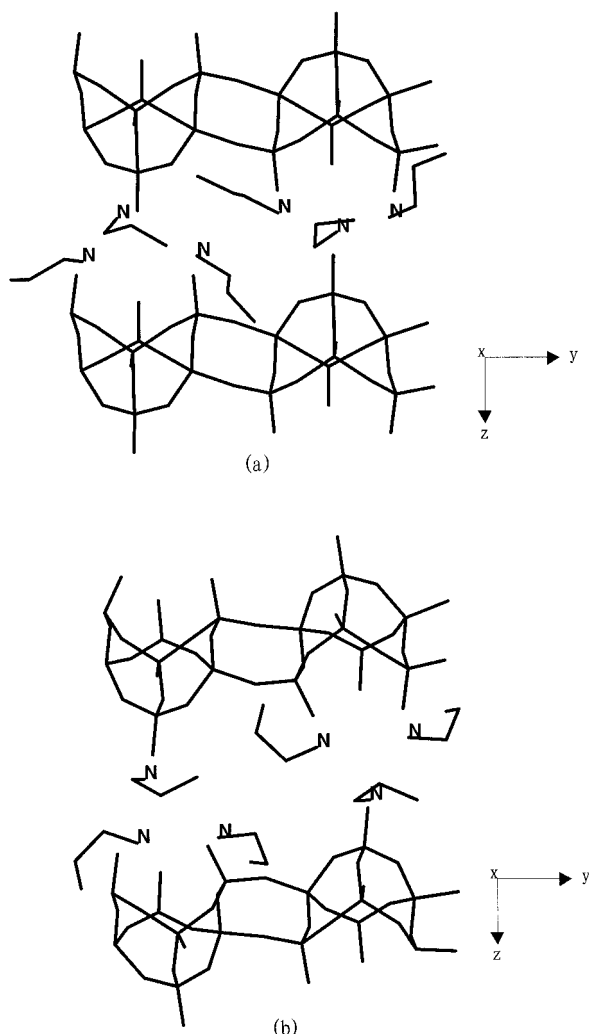


Figure 3. (a) Theoretical template $\text{CH}_3\text{CH}_2\text{CH}_2\text{NH}_2$ (T-2) packing in the interlayer region of the sheets of **L-2** and (b) experimental template $\text{CH}_3\text{CH}_2\text{CH}_2\text{NH}_2$ packing in the interlayer region of **L-4**.

and host network is omitted). It is assumed that $E_{\text{inter}} = E - E_s - E_R$, where E is the total energy of the whole structure, E_s is the steric energy of the framework, and E_R is the energy of organic template itself. An interaction energy E_{inter} including the energies of van der Waals (VDW) and H-bond can then be calculated. The calculated E_s , E_{inter} , and their components of **L- n** ($n = 1-11$) are listed in Tables 2 and 3, respectively.

The calculated experimental E_s values of **L- n** ($n = 1-7$, and 9) in Table 2 are similar. The energy difference between them is lower than 7.0 kcal/mol. **L-8**, **L-10**, and **L-11** exhibit relatively higher E_s value. The E_s value of **L-8** is much higher than that of others, this is because its experimental layer is more highly puckered than any other normal 2D nets. The bond angles at the bridging oxygens (Al–O–P 131.2–175.6°) in **L-8** vary more widely than those of other sheets (typically, av Al–O–P 140°). As a consequence its Bond and Urey–Bradly energies are much higher as compared with others. As with **L-8**, the E_s values of **L-10** and **L-11** are also high due to their high bond and Urey–Bradly values.

The results in Table 3 show that the interaction energies of **L- n** vary from –11.49 to –33.22 kcal/mol, with the exception of **L-8** and **L-11** which exhibit higher

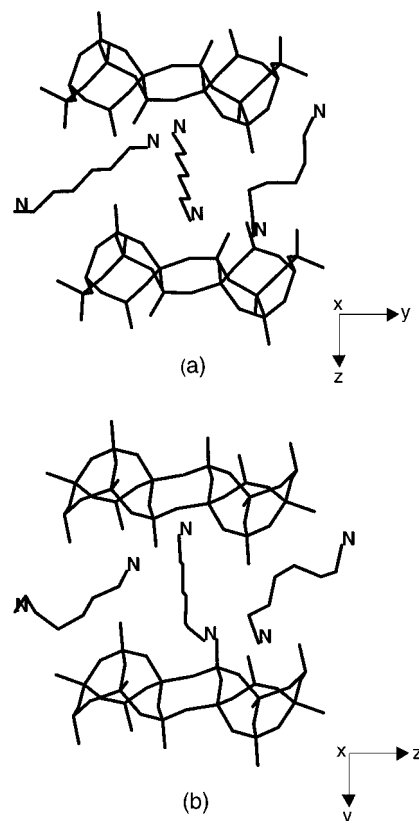


Figure 4. (a) Theoretical template 1,6-hexanediamine (T-13) packing in the interlayer region of the sheets of **L-2** and (b) experimental template 1,6-hexanediamine packing in the interlayer region of **L-12**.

interaction energies of –4.51 and –4.10 kcal/mol, respectively. As we have noted before, H-bonding between the inorganic networks and the templates can stabilize the 2D layered structures. The van der Waals interaction is often an unfavorable factor in these structures as noted in Table 3. This is because the template molecules need to exist in a special geometrical configuration so as to favor the formation of H-bonds to the inorganic sheets.

The experimental interlayer spacing (D) of **L- n** given in Table 3 shows that the separation of two adjacent inorganic layers does not change very much for those layered compounds with the same structures while directed by different templates with various sizes and shapes. For instance, the interlayer spacing of **L- n** ($n = 2-5$) are within the range of 9.363–9.799 Å. This means that the size and shape of template molecules do not affect the interlayer spacing very much.

2. Investigating the Templating Ability of Various Organic Amines for Experimental Inorganic Networks. In terms of the optimized interaction energy of host–template, we shall determine whether a template molecule can stabilize a particular experimental layer structure. To validate our methodology, the sheet of compound **L-2**, a 4.6.8(a) network with an AAAA stacking sequence is tested. First, $\text{C}_2\text{H}_5\text{NH}_3^+$ cations are located in the interlayer region according to the procedure described in the Methodology section and the optimized interaction energy of host–template is calculated. The results from computation are listed in Table 4 and are compared with experimental data. It can be seen that the calculated results using our method are

in good agreement with the optimized experimental data. The interlayer spacing of **L-2**_(test1) and **L-2**_(opt) is very similar, which does not change very much compared with the experimental interlayer spacing of **L-2**. It is worth noting that if the template molecules are randomly located in the interlayer region as in **L-2**_(test2), the modeling cannot give rise to a reasonable model like the experimental structure. Even though energy optimization for **L-2**_(test2) can give a lower energy comparable to the energy of **L-2**_(opt), the H-bond interaction between the templates and the host in **L-2**_(test2) is not reasonable at all. This suggests that the theoretical templates must be located in terms of the H-bonding interaction regularity as discussed before so as to make the prediction reasonable.

Furthermore, some typical theoretical organic amines including mono-, di-, and cycloamines were chosen to investigate their templating abilities for seven different compounds with $\text{Al}_3\text{P}_4\text{O}_{16}^{3-}$ stoichiometry. The optimized interaction energies of the host inorganic sheets and templates are listed in Table 5.

From the calculation results, it is found that the experimental structures have lower host-template interaction energies with a range from -37.07 to -29.02 kcal/mol. This means that experimental template-host network combinations are energetically favorable. On comparing the interaction energies of a given template with different inorganic networks, some experimental phenomena can be explained. For instance, when $\text{C}_2\text{H}_5\text{NH}_2$ (T-1) is used as a template for a 4.6.8(a)-net, an experimental AAAA stacking in **L-2** is more favorable than a hypothetical ABAB stacking in **L-1**. Similarly, when $\text{C}_4\text{H}_9\text{NH}_2$ (T-4) is used as a template, the structure of a 4.6.12-net is more stable than that of a 4.6.8(a) net; moreover, the 4.6.12-net is favored by an experimental AAAA stacking over a hypothetical ABAB stacking. In contrast, using $\text{H}_2\text{NC}_4\text{H}_8\text{NH}_2$ (T-9) as a template, the structure of a 4.6.12 net is stabilized more by an experimental ABAB stacking in **L-6** than a hypothetical AAAA stacking. In addition, calculation results demonstrate that using mixed templates $\text{H}_2\text{NC}_5\text{H}_{10}\text{NH}_2/\text{C}_5\text{H}_{10}\text{N}$ (T-14) in **L-3** or $\text{C}_5\text{H}_{10}\text{NH}/2\text{C}_4\text{H}_7\text{NH}_2$ (T-16) in **L-5** for the experimental 4.6.8(a)-net with an AAAA stacking sequence is more energetically favorable than using solely $\text{H}_2\text{NC}_5\text{H}_{10}\text{NH}_2$ (T-10), $\text{C}_5\text{H}_{10}\text{N}$, or $\text{C}_4\text{H}_7\text{NH}_2$ (T-15) as a template. This explains the incorporation of two different organic ammonium cations between aluminophosphate layers. Similarly, the structure of **L-1** is more stable when $^+\text{H}_3\text{NC}_2\text{H}_4\text{NH}_3^+$ and $\text{OHC}_2\text{H}_4\text{OH}_2^+$ cations both interact with the inorganic network through H-bonding.

Furthermore, some suitable templates can be predicted that have lower interaction energies with a given inorganic network as indicated by data in italics in Table 5. For example, if the experimental sheets of **L-2** are chosen as a host, calculation result gives that the interaction energy of **L-2** and T-2 is -33.27 kcal/mol,

which is close to the optimized experimental E_{inter} value of -33.11 kcal/mol. Therefore $\text{CH}_3\text{CH}_2\text{CH}_2\text{NH}_2$ (T-2) is a suitable template, stabilizing the sheets of **L-2**. Figure 3a shows the predicted position of T-2 in the interlayer region of **L-2**. The predicted template position and the manner of H-bonding interaction in the theoretical structure are in agreement with those in the experimental structure of **L-4** as shown in Figure 3b, even though there are some differences between the theoretical and experimental configurations of the templates.

Another example is that 1,6-hexanediamine (T-13) is predicted to be a suitable template for the formation of the 4.6.8(a)-net sheet of **L-2**. The calculated interaction energy of **L-2** and T-13 is -31.68 kcal/mol. This value is close to the optimized experimental interaction energy of -33.11 kcal/mol in **L-2**. Therefore, 1,6-hexanediamine is predicted to be able to stabilize the sheets of **L-2**. This is confirmed by the experimental fact that 1,6-hexanediamine can direct the formation of the 4.6.8(a)-net sheets of **L-12** [$\text{Al}_3\text{P}_4\text{O}_{16}$] $1.5[\text{NH}_3(\text{CH}_2)_6\text{NH}_3]$ (*P1*, $a = 8.952$ Å, $b = 9.381$ Å, $c = 14.840$ Å, $\alpha = 91.87^\circ$, $\beta = 91.46^\circ$, and $\gamma = 102.39^\circ$). Figure 4a shows the theoretical template 1,6-hexanediamine packing in the interlayer region of the sheets of **L-2**. The predicted template position and the manner of H-bonding interaction in the theoretical structure are in good agreement with those in the experimental structure of **L-12** (Figure 4b).

Our further work is focusing on prediction of suitable templates for a variety of theoretical 2D nets using this method.

Conclusions

In this paper, the structural features of a series of 2D layered aluminophosphates with $\text{Al}_3\text{P}_4\text{O}_{16}^{3-}$ stoichiometry are discussed. These compounds are templated by various template agents, such as chainlike monoamines, diamines, and cycloamines. The interaction of the inorganic layers (mainly described as the secondary building units) and the templates are dominated by H-bonds with certain regularities, which allows the template molecules in the interlayer region of a 2D layer structure to be located with reasonable success. In terms of energy calculation, the steric energy and the interaction energy between the template and the inorganic host could be determined and the results can further explain the templating ability of various organic amines for the experimental 2D structure. Calculations can predict the suitable templates for the given 2D nets correctly, thus making our methodology a powerful new tool in the rational design and synthesis of desired target materials.

Acknowledgment. This research is supported by Pan Deng Foundation Project of China.

CM990289N